

# Optimal Determination of the Vapor Pressure Critical Exponent

CLIFFORD W. WALTON

JOSEPH C. MULLINS

JAMES C. HOLSTE

KENNETH R. HALL

and

PHILIP T. EUBANK

Department of Chemical Engineering  
Texas A&M University  
College Station, Texas 77843

Correlations producing thermodynamic property tables employ the concepts of scaling with increasing frequency in the vapor-liquid critical region. One of the important concepts is that the vapor pressure equation should provide infinite curvature and finite slope  $\psi_c$  at the critical point. The vapor pressure critical exponent  $\theta$  describes the divergent curvature in a power law expression.

This paper provides an extensive study of  $\theta$ . We have determined an optimal value of  $\theta$  by two general approaches: a curve fit method (CFM) which employs least-squares analyses, and a numerical derivative method (NDM). The CFM is interpolative but requires a vapor pressure equation, while the NDM is extrapolative but is independent of the vapor pressure equation.

The vapor pressure equations, which satisfy scaling concepts most closely, exhibit a very flat minima for the CFM. As a result, the values of  $\theta$  which provide reasonable correlations vary over an appreciable range (depending upon the compound, form of the equation, and the temperature range). The NDM did not present any particular difficulties. Our overall weighted average for  $\theta$  is 0.199 with a standard deviation of 0.052, while the overall numerical average was 0.225 with a standard deviation of 0.045; the final recommended value of  $\theta$  is  $0.22 \pm 0.04$ .

## SCOPE

Scaling theory predicts a nonanalytic vapor pressure equation in which the vapor pressure critical exponent  $\theta$  characterizes divergent curvature (Stanley, 1971). Non-analytical vapor pressure equations (which include  $\theta$ ) have increased the accuracy of correlating vapor pressure data, especially near the critical point (CP). The question of whether  $\theta$  is the same for all compounds (universal) is basic to understanding the behavior of real fluids. Values of  $\theta$  abound in the literature ranging from zero (Kierstead, 1971) to 0.5 (Goodwin, 1969), while scaling theory predicts about 0.1 (Vicentini-Missoni et al., 1969; Widom and Rowlinson, 1970) when the variables of chemical potential and temperature are mixed. Scaling in the mixed variables of pressure, temperature, and chemical potential, however, predicts  $\theta = \alpha + \beta \cong 0.47$ .

The general objectives of this work are to present a definitive study of  $\theta$ , to explain the differing literature values, to determine the factors upon which  $\theta$  depends, and to

select the best, present value complete with error band from the available data. Factors considered were: general method for  $\theta$  determination, selection of a vapor pressure equation (when required by the method), temperature range of the data, and variation of the critical temperature and pressure. Our objective was not to fit accurately vapor pressure data from the triple point to the critical point with a minimum number of parameters; a companion project (Nuchols, 1976) had that goal.

Specifically, optimum values of  $\theta$  were obtained by two general methods: a curve fit method (CFM) and a numerical derivative method (NDM). The CFM requires minimization of an objective function which contains an assumed vapor pressure equation. Two minimization techniques were employed: nonlinear least squares (NLS) and maximum likelihood (ML). The NDM, presented for the first time, does not require the assumption of a vapor pressure equation.

Power law equations derived from the scaling hypothesis are only asymptotically valid approaching the CP; therefore, unsmoothed vapor pressure data of high precision with a minimum of ten points within 10% of the critical temperature are necessary for analysis. The substances studied were carbon dioxide, ethane, ethylene, helium-4, methane, oxygen, and water.

Correspondence concerning this paper should be addressed to Philip T. Eubank. Clifford W. Walton is with the U.S. Army Corps of Engineers, Ft. Belvoir, Virginia. Joseph C. Mullins is on sabbatical leave from the Department of Chemical Engineering, Clemson University, Clemson, South Carolina.

## CONCLUSIONS AND SIGNIFICANCE

The vapor pressure critical exponent  $\theta$  from this work appears to have a universal value of  $0.22 \pm 0.04$ . Variations in  $\theta$  reflect the temperature range of the data and the assumed forms of the vapor pressure equation. The exponent was less sensitive to the general method of calculation and small variations of critical temperature along the vapor pressure/critical isochore curve.

The broad minimum of the least-squares objective function minimized by the curve fit method appears to be the

major reason for the variation in  $\theta$  (0 to 0.50) found in recent literature. Values of  $\theta$  in the range 0 to 0.50 will adequately represent individual data sets for individual vapor pressure equations for carbon dioxide, helium-4, methane, oxygen, and water within experimental accuracy. Highly precise data, such as those for ethylene and ethane, produce a range of  $\theta$  from 0.1 to 0.3 for various individual equations.

The similarity of physical behavior in the critical region of the various types of phase transitions led to the scaling theory, a sophisticated corresponding states approach which uses two scale factors as the independent field variables. All the critical exponents are then universal, but two amplitudes in the many power laws are system dependent. A readable account of scaling and universality has been recently published (Levelt Sengers, et al., 1977).

Simple scaling theory (Stanley, 1971) predicts a divergence of the second derivative of the vapor pressure with respect to temperature at the critical point CP as

$$(d^2P_{\sigma R}/d\tau^2) \sim \tau^{-\theta}, \quad (\tau \geq 0) \quad (1)$$

where  $\tau \equiv 1 - T/T_c$  and  $P_{\sigma R} = P_{\sigma}/P_c$ . Positive values of  $\theta$  obtained from experimental data verify this divergence from the two-phase side of the CP. Simple scaling theory also predicts infinite curvature at the CP for the critical isochore ( $\tau \leq 0$ ), but this anomaly has been neither verified nor disproved experimentally. Indeed, the single-phase, critical isochore appears to be very straight in the critical region (or  $\theta^+ = 0$ ) (Rowlinson, 1958; Vicentini-Missoni et al., 1969).

To prevent divergence of the second temperature derivative of chemical potential at the CP, the Yang-Yang identity (Yang and Yang, 1964) and simple scaling theory also require that  $\theta$  equals  $\alpha$ , the analogous critical exponent for divergence of the isochoric heat capacity  $C_V$ . Experimental measurements of  $C_V$  along the critical isochore do show divergence with the same exponent as the CP is approached from either the single- or two-phase side. Measurements in the past decade have generally provided values of  $\alpha$  between 0.10 and 0.15 in agreement with the theoretical value of ( $1/8$ ) from the three-dimensional Ising model of the lattice gas.

Disagreements with the simple scaling result  $\theta = \alpha = (1/8)$  have recently arisen in the literature. First, Hall and Eubank (1976) found  $(1-2\beta)$ , a value definitely greater than  $1/8$ , to be a lower bound of  $\theta$  by applying the Clapeyron identity to empirical equations supported by experiment in the critical region ( $\beta$  is the critical exponent related to the coexisting phase density differences). Second, Goodwin (1975), Baehr et al. (1976), and Wagner et al. (1976) have found  $\theta$  to be 0.5 (or higher) while fitting their various nonanalytic vapor pressure equations. These higher values ( $\theta > 0.5$ ) conflict with a critical exponent inequality derived from thermodynamics by Griffiths (1967):

$$\theta \leq \alpha + \beta \quad (2)$$

where  $\alpha + \beta \approx 0.5$  (max).

Revised scaling theory (Rehr and Mermin, 1973) does not change the contention that  $\theta$  equals  $\alpha$  because the two scaling variables are linear combinations of a temperature variable  $\tau$  and a chemical potential variable  $\Delta\mu_R \equiv (\mu_c - \mu)/RT_c$ . Further revisions of the theory to allow scaling variables that are linear combinations of  $\tau$ ,  $\Delta\mu_R$  and a pressure variable  $(P_c - P)/P_c$  can provide  $\theta = \alpha + \beta \approx 0.5$  (max) (Nicoll et al., 1975).

## THE VAPOR PRESSURE EQUATIONS

Because Equation (1) applies asymptotically upon approaching the CP, a series of correction terms are required to correlate vapor pressure data over any finite temperature range immediately below  $T_c$ :

$$(d^2P_{\sigma R}/d\tau^2) = C_1\tau^{-\theta}(1 + c_2\tau^\eta + \dots) \quad (3)$$

Truncation after one correction term leaves

$$(d^2P_{\sigma R}/d\tau^2) = C_1\tau^{-\theta} + C_2\tau^{\eta-\theta} \quad (4)$$

which becomes upon integration

$$(dP_{\sigma R}/d\tau) = -\psi_c + C_1(1-\theta)^{-1}\tau^{1-\theta} + C_2(1+\eta-\theta)^{-1}\tau^{1+\eta-\theta} \quad (5)$$

and

$$P_{\sigma R} = 1 - \psi_c\tau + C_1(1-\theta)^{-1}(2-\theta)^{-1}\tau^{2-\theta} + C_2(1+\eta-\theta)^{-1} \times (2+\eta-\theta)^{-1}\tau^{2+\eta-\theta} \quad (6)$$

where the slope of the critical isochore at the CP

$$\psi_c \equiv (T_c/P_c)(\partial P/\partial T)_{\rho_c}|_{T=T_c} = -(dP_{\sigma R}/d\tau)|_{\tau=0} \quad (7)$$

and unity are the constants of integration. The extended scaling value of  $\eta$  is 0.5 (Wegner, 1972), while the linear term  $1 - \psi_c\tau$  is an analytical background. Equation (6), which contains a minimum, necessary background, can be generalized as

$$P_{\sigma R} = D_0(\tau) + E_0\tau^{2-\theta} + F_0\tau^{2+\eta-\theta} \quad (8)$$

where  $D_0(\tau)$  is any analytic function of temperature such that  $D_0(0) = 1$ , and the first derivative  $\underline{D_0}'(\tau)$  has the limit  $\underline{D_0}'(0) = -\psi_c$ .

For example, the vapor pressure equation of Hastings and Levelt Sengers (1977) assumes  $F_0 = 0$  and a cubic polynomial for  $\underline{D_0}(\tau)$  or

$$P_{\sigma} = D_1 + D_2\tau + D_3\tau^2 + D_4\tau^3 + E\tau^{2-\theta} \quad (9)$$

where  $D_1 = P_c$  and  $D_2 = -\psi_c P_c$ . Differentiation of Equation (9) followed by rearrangement to a form similar to that of Equation (3) provides

$$(d^2P_{\sigma R}/d\tau^2) = E^*\tau^{-\theta}(1 + D_3^*\tau^\theta + D_4^*\tau^{1+\theta}) \quad (10)$$

where  $E^* = (2 - \theta)(1 - \theta)E$ ,  $D_3^* = 2D_3/E^*$ , and  $D_4^* = 6D_4/E^*$ .

## PROCEDURE

### Curve Fit Method (CFM)

We fit vapor pressure data to specific equations by nonlinear least-squares analysis and maximum likelihood. The first technique consists of a linearization of the objective function (or variance)

$$\sum W(\Delta P)^2 \equiv (N - M)^{-1} \sum_{i=1}^N [W(P_{\sigma} - P_{eq})^2]_i \quad (11)$$

We used the Gauss-Newton method as described by Hust and McCarty (1967) and Gielen et al. (1973). Walton (1977) lists the computer program VAPPRESS. When convergence failed for a number of the data sets, a direct search established the nonlinear parameters  $\theta$  and  $\eta$ .

One vapor pressure equation was Equation (6), written as

$$P_{\sigma R} - 1 = {}^1A_1\tau + {}^1A_2\tau^{1A_3} + {}^1A_4\tau^{(1A_3+1A_5)} \quad (12)$$

where  ${}^1A_1 = -\psi_c$ ,  ${}^1A_3 = 2 - \theta$ , and  ${}^1A_5 = \eta$ . Although repetitious, we carefully rewrite here the vapor pressure equations of the previous section using  ${}^kA_j$  to denote free (adjustable) parameters found by minimization of the objective function. Any parameters other than  ${}^kA_j$  (such as  $\theta$  and  $\eta$ ) which appear explicitly in the following equations are input as constant values and are not adjusted. For example, the constants  ${}^1A_1 - {}^1A_5$  were determined from minimization of the objective function for Equation (12) holding  $T_c$  and  $P_c$  fixed at their experimental values. When convergence failed,  $P_c$  was allowed to float by fitting

$$P_{\sigma} = {}^2A_1\tau + {}^2A_2\tau^{2A_3} + {}^2A_4\tau^{(2A_3+2A_5)} + {}^2A_6 \quad (13)$$

where  ${}^2A_6$  is the computed value of  $P_c$ , and  $\psi_c = -{}^2A_1/{}^2A_6$ .

When Equation (13) failed to converge, we mapped the objective function vs.  $\theta$  and  $\eta$  by linear fits of the equation

$$P_{\sigma} = {}^3A_1\tau + {}^3A_2\tau^{2-\theta} + {}^3A_4\tau^{2+\eta-\theta} + {}^3A_6 \quad (14)$$

for chosen values of  $\theta$  and  $\eta$ .

Results from Equation (14) indicated that the higher-order, nonlinear term is often unnecessary, so we also studied equations corresponding to (13) and (14):

$$P_{\sigma} = {}^4A_1\tau + {}^4A_2\tau^{4A_3} + {}^4A_4 \quad (15)$$

and

$$P_{\sigma} = {}^5A_1\tau + {}^5A_2\tau^{2-\theta} + {}^5A_4 \quad (16)$$

Equation (9) was studied in the forms

$$P_{\sigma} = {}^6A_1\tau + {}^6A_2\tau^{6A_3} + {}^6A_4\tau^2 + {}^6A_5\tau^3 + {}^6A_6 \quad (17)$$

and

$$P_{\sigma} = {}^7A_1\tau + {}^7A_2\tau^{2-\theta} + {}^7A_4\tau^2 + {}^7A_5\tau^3 + {}^7A_6 \quad (18)$$

### Numerical Derivative Method (NDM)

Close to the CP, the higher-order, nonlinear term of Equation (5) becomes negligible, leaving

$$(dP_{\sigma R}/d\tau) = C_1(1 - \theta)^{-1}\tau^{1-\theta} - \psi_c \quad (19)$$

or

$$\ln(\psi_c + dP_{\sigma R}/d\tau) = (1 - \theta)\ln\tau + \ln C_1(1 - \theta)^{-1} \quad (20)$$

Within the temperature range  $0 \leq \tau \leq 0.1$ , Equation (20) yields a straight line with slope  $(1 - \theta)$  when  $\ln(\psi_c + dP_{\sigma R}/d\tau)$  is graphed against  $\ln\tau$ .

Numerical derivatives ( $dP_{\sigma R}/d\tau$ ) result from application of various central and end point derivative formulas (Hildebrand, 1974) to vapor pressure values interpolated on even temperature intervals by the iterative Lagrangian procedure (Moursund and Duris, 1967). A nine point central difference formula was used, when possible, to obtain accurate derivatives. Because of the precision of the various data sets, little fluctuation was observed in the derivatives; central difference with fewer points agreed roughly with the derivatives from the nine point formula. Next, we used these derivatives as input for a weighted least-squares analysis (Young, 1962) of Equation (20), rewritten as

$$\ln(\psi_c + D_R) = B_1\ln\tau + B_2 \quad (21)$$

An optimum value of  $\psi_c$ ,  $\psi_{co}$ , was found by varying  $\psi_c$  for repetitive fits of Equation (21) until the minimum of the sum of the weighted, squared deviations of  $\ln(\psi_c + D_R)$  resulted. The optimum value of  $\theta$  then equals  $(1 - B_1)$  for  $\psi_c = \psi_{co}$ . Walton (1977) provides the computer program NUMDVFIT.

### Weighting Factor

Levelt Sengers (1970) notes that "experimental points have to be carefully weighted to allow for diminishing precision when the CP is approached." This increase of experimental error arises largely from the increasing importance of gravitational effects which create large density gradients in the sample. Restricting the height of the cell to about 1 cm diminishes these density and pressure gradients.

TABLE 1. VAPOR PRESSURE DATA SOURCES

Compound identification	Vapor pressure data reference	Critical point reference
Carbon dioxide A	Levelt Sengers and Chen (1972)	Moldover (1974)
Carbon dioxide B	Levelt Sengers and Chen (1972)	Levelt Sengers and Chen (1972)
Ethane	Douslin and Harrison (1973)	Douslin and Harrison (1973)
Ethylene A	Douslin and Harrison (1976)	Douslin and Harrison (1976)
Ethylene B	Hastings and Levelt Sengers (1977)	Moldover (1974)
Helium A	Roach (1968)	Roach (1968)
Helium B	Kierstead (1971)*	Kierstead (1971)
Methane	Prydz and Goodwin (1972)	Jansoone et al. (1970)
Oxygen A	Hoge (1950)	Hoge (1950)
Oxygen B	Wagner et al. (1976)	Wagner et al. (1976)
Water A	Osborne et al. (1933)	Osborne et al. (1939)
Water B	Osborne et al. (1933)	Blank (1969)

\* Measured first derivatives of the vapor pressure.

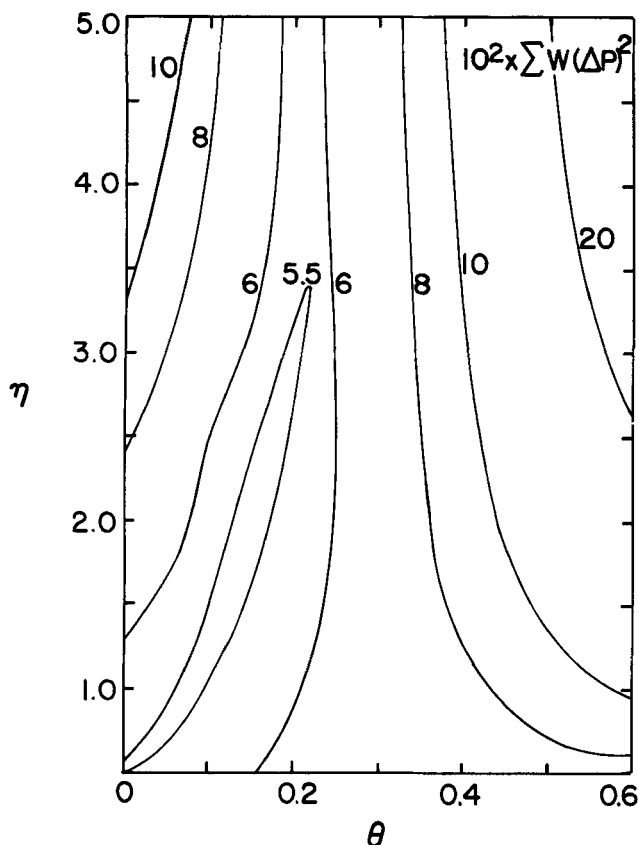


Fig. 1. Objective function contours for Equation (14) with carbon dioxide A.

In this work, the assumption of normally distributed relative error in the pressure measurements leads to

$$W_i = [(P_{\sigma R,i} - 1)/P_{\sigma R,i}]^2 \quad (22)$$

This weighting factor agrees with the observation of Verbeke (1970) that the errors in pressure in the critical region depend on  $(P_c - P_\sigma)$  rather than  $P_\sigma$  alone.

#### Data Selection

The leading anomalous term  $\tau^{2-\theta}$  of Equation (6) is of high order; thus accurate values of  $\theta$  cannot be extracted from extremely narrow temperature bands below  $T_c$ . The asymptotic range is small, however, and a range large enough to include significant contributions from the  $\tau^{2-\theta}$  term will also include contributions from still higher-

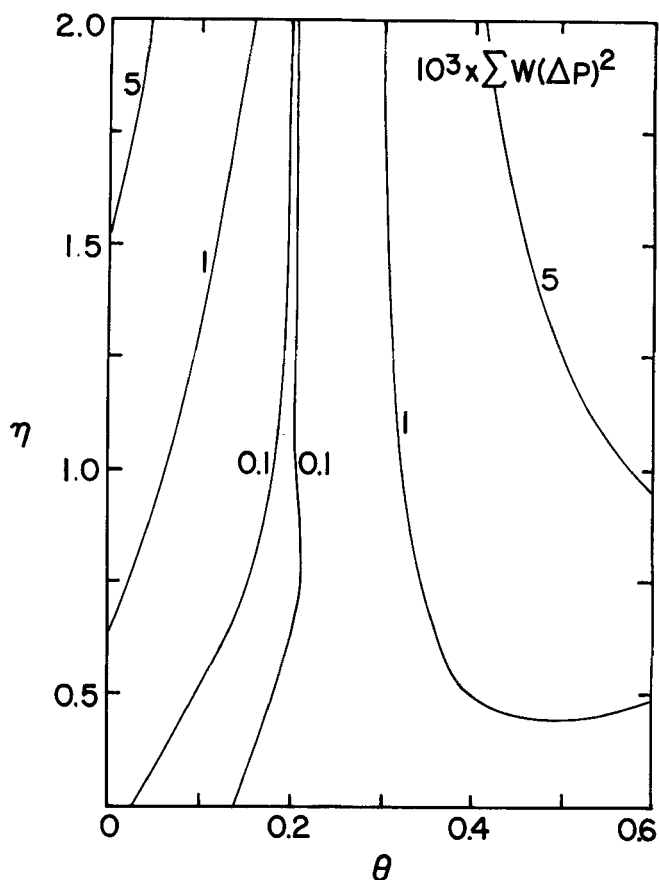


Fig. 2. Objective function contours for Equation (14) with ethane.

order terms such as  $\tau^{2+\eta-\theta}$  (Hastings and Levelt Sengers, 1977).

The experimental data chosen were those with the most precise, unsmoothed values available with a minimum of ten points in the temperature range considered:  $0 \leq \tau \leq 0.1$ . The seven different compounds with ten different data sets were labeled as in Table 1 to account, in some cases, for different fixed values of  $T_c$  and  $P_c$ . All units have been converted to SI. No adjustment has been made for the different temperature scales except for methane and water B, where the critical temperature is adjusted to match the scale of the vapor pressure data. A detailed discussion of gravitational errors is beyond the scope of this manuscript; fortunately, considerable literature is available (Kim et al., 1974; Yang et al., 1977).

TABLE 2. CONVERGED NLS RESULTS FOR ETHYLENE A\*  
Experimental values:  $T_c = 282.35$  K  $P_c = 5\,041.97$  kPa

(Equation)/data points temperature range	(12)/13 $0 < \tau \leq 0.086$	(13)/13 $0 < \tau \leq 0.086$	(17)/13 $0 < \tau \leq 0.086$	(15)/13 $0 < \tau \leq 0.086$
$\theta$ ( $\sigma_\theta$ )	0.208 (0.004)	0.175 (0.015)	0.120 (0.046)	0.258 (0.003)
$\psi_c$ ( $\sigma_\psi$ )	6.370 (0.002)	6.353 (—)	6.350 (—)	6.426 (—)
Max. absolute % dev.	0.004	0.001	0.001	0.025
Avg. absolute % dev.	0.001	<0.001	<0.001	0.010
$\sigma_P$ , kPa	0.1248	0.0309	0.0353	0.8461
$\Sigma W(\Delta P)^2$ , (kPa) $^2 \times 10^6$	1.7	0.56	0.59	133
$A_1$ ( $\sigma_1$ )	-6.3695646 (0.002)	-32 028.219 (32)	-32 013.824 (32)	-32 405.999 (32)
$A_2$ ( $\sigma_2$ )	9.5355451 (0.12)	53 612.906 (3200)	97 197.674 (48000)	43 575.987 (143)
$A_3$ ( $\sigma_3$ )	1.7917923 (0.004)	1.8249188 (0.015)	1.8796755 (0.046)	1.7415751 (0.003)
$A_4$ ( $\sigma_4$ )	-6.4224926 (1.9)	-22 303.976 (817)	-41 332.797 (51000)	5 043.1001 (0.24)
$A_5$ ( $\sigma_5$ )	1.5476244 (0.24)	0.83294414 (0.21)	-17 090 259 (5100)	—
$A_6$ ( $\sigma_6$ )	—	5 041.7372 (0.061)	5 041.7267 (0.066)	—

\* Values for the  $A_i$  are reported to eight digits to allow reproduction of our fits only.

TABLE 3. EFFECT OF TEMPERATURE RANGING FOR ETHYLENE A USING EQUATION (15)\*

Temperature range Number of data points	$0 < \tau \leq 0.086$ 13	$0 < \tau \leq 0.068$ 12	$0 < \tau \leq 0.050$ 11	$0 < \tau \leq 0.033$ 10	$0 < \tau \leq 0.015$ 9	$0 < \tau \leq 0.012$ 8
$\theta$ ( $\sigma_\theta$ )	0.258 (0.003)	0.241 (0.003)	0.218 (0.001)	0.221 (0.004)	0.179 (0.006)	0.179 (0.016)
$\psi_c$	6.426	6.399	6.371	6.373	6.354	6.354
Max. % deviation	0.0249	0.0122	0.0017	0.0021	0.0007	0.0007
Avg. abs. % dev.	0.0099	0.0050	0.0007	0.0008	0.0002	0.0002
$\sigma_{P_{eq}}$ kPa	0.846	0.430	0.064	0.181	0.017	0.019
$\Sigma W(\Delta P)^2$ , (kPa) <sup>2</sup> $\times 10^6$	133	20	0.15	0.16	0.017	0.021
$A_1$ ( $\sigma_1$ )	-32 406 (32)	-32 267 (22)	-32 123 (5)	-32 132 (17)	-32 037 (13)	-32 037 (28)
$A_2$ ( $\sigma_2$ )	43 575 (143)	44 628 (162)	46 444 (60)	46 206 (466)	52 234 (913)	52 195 (2655)
$A_3$ ( $\sigma_3$ )	1.742 (0.003)	1.759 (0.003)	1.782 (0.001)	1.779 (0.004)	1.821 (0.006)	1.821 (0.016)
$A_4$ ( $\sigma_4$ )	5 043.1 (0.2)	5 042.4 (0.1)	5 041.9 (<0.1)	5 041.9 (<0.1)	5 041.8 (<0.1)	5 041.8 (<0.1)

\* The values of the  $A_i$  listed here only demonstrate size and cannot be used to reproduce results using Equation (15).

## RESULTS

## Curve Fit Method

**Nonlinear Least-Squares Technique (NLS).** Initial attempts to minimize the objective function with Equation (13) failed. Next, Equation (14) was used to calculate the objective function at fixed values of  $\theta$  and  $\eta$ , with the remaining parameters determined by linear least squares. Repetition at incremented values of  $\theta$  and  $\eta$  produced a three-dimensional surface for the objective function for carbon dioxide A, ethane, ethylene A, ethylene B, helium A, methane, oxygen A, oxygen B, and water B. The supplemental tables contain values of the objective function for  $\theta$  ranging from zero to 0.6 at 0.1 intervals, with  $\eta$  ranging from 0.1 to about 0.8, depending upon the compound.

These surfaces were of two classes. The first and larger class possessed flat error surfaces as illustrated by Figure 1 for carbon dioxide A. The objective function changed less than two orders of magnitude while  $\theta$  was varied over its full range. This class also included helium A, methane, oxygen A, oxygen B, and water B, although the latter exhibited somewhat larger variations. The second class, which included ethane, ethylene A, and ethylene B, was characterized by steep error surfaces with variations over five orders of magnitude in the objective function as shown in Figure 2 for ethane.

The asymptotic value of  $\theta$  immediately at the CP could be found theoretically from the infinite series form of Equation (14):

$$P = P_c + A_1\tau + \tau^{2-\theta} \cdot \left[ \sum_{i=0}^{\infty} A_{i+2}\tau^{i\eta} \right] \quad (23)$$

We have found the optimum value of  $\theta$  to be about 0.22 when the series of Equation (23) is set to unity. The addition of a second term in the series [that is, Equation (14)] provides the contours of Figures 1 and 2. It is obvious from these contours that  $\theta$  and  $\eta$  are highly cross correlated so that the asymptotic value of  $\theta$  cannot be found from even our most precise vapor pressure data at present.

The minima obtained from these searches then were used as starting values of  $\theta$  and  $\eta$  to provide global minima for Equation (13) for ethane, ethylene A, ethylene B, and methane. The other data sets did not converge. For these sets, various values of  $\theta$ , with  $\eta$  corresponding to a near minimum in the objective function, were used to determine the fit of the data. These unconverged results are in the supplement with values of  $\theta$  ranging from 0.0 to 0.6.

Similar one-dimensional searches were performed at various fixed values of  $\theta$  for Equations (16) and (18). The value of  $\theta$  minimizing the objective function was then used in the general form of these equations, Equations (15) and (17), respectively. Only ethylene A converged to a possible value of  $\theta$  for Equation (17), while Equation (15) converged to a reasonable solution for all compounds analyzed.

Tables 2 and 3 give the complete NLS-CFM results for ethylene A with  $\eta = 1.34$  ( $\sigma_\eta = 0.24$ ) by Equation (12) and  $\eta = 0.65$  ( $\sigma_\eta = 0.23$ ) by Equation (13), with  $\sigma$  being the standard deviation. A summary of NLS results for the substances of Table 1 is given in Table 4. NLS did not produce meaningful results for carbon dioxide B, helium B, and water A for any of the equations. Table 7 contains weighted average values of  $\theta$  and  $\sigma_\theta$  from the various converged equations by NLS. The weighting factor was the inverse square of the standard deviation or  $\sigma_\theta^{-2}$ .

TABLE 4. SUMMARY OF NLS RESULTS FOR THE VARIOUS SUBSTANCES

Substance	Equation	Least-squares fit results							Experimental	
		$\theta$	$\sigma_\theta$	$\tau_{\max}$	# points	$\eta$	$\sigma_\eta$	$\psi_c$	$P_c$	$T_c$
Carbon dioxide A	(13)	Did not converge							7 375.3	304.127
	(15)	0.295	0.016	0.095						
		0.263	0.011	0.049						
Ethane		0.123	0.034	0.020					4 871.76	305.33
	(12)	0.1702	0.0066	0.089	10	0.646	0.097			
	(13)	0.127	0.031	0.089	10	0.646	0.097	6.427		
	(15)	0.2677	0.0047	0.089						
		0.2503	0.0040	0.073						
		0.2306	0.0022	0.056						
Ethylene A	(17)	Did not converge							5 041.97	282.35
	(12)	0.208	0.004	0.086	13			6.370		
	(13)	0.175	0.015	0.086	13			6.353		
	(17)	0.120	0.046	0.086	13			6.350		
	(15)	0.258	0.003	0.086	13			6.426		
		0.241	0.003	0.068	12			6.399		
		0.218	0.001	0.050	11			6.371		
		0.221	0.004	0.033	10			6.373		
		0.179	0.006	0.015	9			6.354		
		0.179	0.016	0.012	8			6.354		
	(13)	0.192	0.002	0.157	17			6.358		
	(13)	0.196	0.009	0.157	17			6.362		
	(17)	0.32	22	0.157	17			6.4		
Ethylene B	(12), (17)	Did not converge							5 039.36	282.344
	(13)	0.2217	0.0094	0.086	24	4.2	2.3	6.371		
	(15)	0.2493	0.0031	0.086						
		0.2133	0.0027	0.043						
Helium A	(13)	Did not converge							227.31	5.1888
	(15)	0.093	0.015	0.049						
		0.13	0.20	0.019						
Methane	(13)	0.21	0.15	0.097	21	2.6	12	5.999	4 596.88	190.53
	(15)	0.259	0.012	0.097						
		0.246	0.033	0.071						
		0.226	0.043	0.065						
		0.256	0.057	0.061						
		0.143	0.053	0.055						
		0.217	0.068	0.050						
		0.324	0.083	0.045						
Oxygen A		0.040	0.064	0.040						
	(13)	Did not converge							5 080.8	154.78
	(15)	0.2608	0.0093	0.099						
		0.242	0.028	0.057						
Oxygen B		0.17	0.12	0.030						
	(13)	Did not converge							5 043.0	154.581
	(15)	0.253	0.013	0.094						
		0.144	0.043	0.062						
		0.25	0.040	0.046						
Water B	(15)	0.3379	0.0061	0.099					2 206.2	647.06
		0.2871	0.0076	0.068						
		0.254	0.056	0.018						

**Maximum Likelihood Technique (ML).** The maximum likelihood method of Britt and Luecke (1973) was used to analyze ethane, ethylene A, and ethylene B data. The other compounds were omitted owing to computer expense. Briefly, maximum likelihood weighting factors are based upon the experimental precisions of both the pressure and the temperature measurements. The results are generally superior to those from NLS. Except for data of extreme precision, however, the degree of improvement does not justify the considerable, additional expense.

Table 5 summarizes the ML results for ethylene A, where Equation (13\*) is the same as Equation (13), except ML determines  $T_c$ . Equation (17) would not converge for ethane and ethylene B despite variation of the temperature range. Convergence was obtained with ethylene A over a wide temperature range ( $\tau \leq 0.157$ ), but the standard deviations  $\sigma_i$  of the coefficients  $A_i$  are equal to

or greater than the respective coefficients. In general, increasing the data range and fixing  $P_c$  and  $T_c$  to the experimental values appears to increase the probability of convergence, decreases the standard deviations of the coefficients, and increases the average absolute percent deviation.

The weighted average results for  $\theta$  by Equations (13), (13\*), and (15) are 0.197 ( $\sigma_\theta = 0.030$ ) for ethane, 0.192 ( $\sigma_\theta = 0.004$ ) for ethylene A, and 0.233 ( $\sigma_\theta = 0.049$ ) for ethylene B. Comparison with the NLS results of Table 7 shows the values of  $\theta$  are in excellent agreement for each data set, but the ML results provide smaller standard deviations except for ethylene B. For each of the data sets of Table 4 not included in the ML analysis, it appears safe to conclude that ML would produce an average  $\theta$  value within one standard deviation of that given in Table 7.

TABLE 5. MAXIMUM LIKELIHOOD RESULTS FOR ETHYLENE A†

Experimental values:  $T_c = 282.35$  K  $P_c = 5\,041.97$  kPa

(Equation)/ data points temperature range	(13)/17 $0 < \tau \leq 0.157$	(13°)/17 $0 < \tau \leq 0.157$	(17)/17 $0 < \tau \leq 0.157$
$\theta$ ( $\sigma_\theta$ )	0.192 (0.002)	0.196 (0.009)	0.32 (29)
$\psi_c$ ( $\sigma_\psi$ )	6.358 (0.001)	6.363 (0.009)	6.4 (5.9)
Max. abs. % dev.	0.001	0.001	0.003
Avg. abs. % dev.	0.0004	0.004	0.001
$\sigma_P$ , kPa	0.021	0.022	0.091
$\sigma_T \times 10^5$ , K	1.3	1.4	4.3
$T_c$ ( $\sigma_{T_c}$ ), K	Exp.	282.40 (0.11)	Exp.
$A_1$ ( $\sigma_1$ )	-32 000 (6)	-32 000 (46)	-32 000 (30 000)
$A_2$ ( $\sigma_2$ )	50 000 (340)	50,000 (1100)	24 000 (360 000)
$A_3$ ( $\sigma_3$ )	1.808 (0.002)	1.804 (0.009)	1.68 (29)
$A_4$ ( $\sigma_4$ )	-27 000 (390)	-27 000 (500)	31 000 (470,000)
$A_5$ ( $\sigma_5$ )	1.236 (0.039)	1.28 (0.1)	-34 000 (180 000)
$A_6$ ( $\sigma_6$ )	5 041.54 (0.01)	5 047 (13)	—

† Values of the  $A_i$  are included for comparative purposes only and will not reproduce results.

TABLE 6. NDM RESULTS FOR ETHYLENE A

Experimental values:  $T_c = 282.35$  K  $P_c = 5\,041.97$  kPa

Data points temperature range	34 $0.002 \leq \tau \leq 0.06$	29 $0.002 \leq \tau \leq 0.05$	24 $0.002 \leq \tau \leq 0.04$	19 $0.002 \leq \tau \leq 0.03$
$\theta$ ( $\sigma_\theta$ )	0.225 (0.003)	0.218 (0.005)	0.213 (0.008)	0.212 (0.017)
$\psi_{co}$	6.375	6.370	6.366	6.365
$\Delta(\psi_{co} + D_R)$				
Avg. abs. % dev.	8.11	6.51	5.16	4.79
Max. abs. % dev.	0.42	0.43	0.49	0.60

Except for Equations (15) and (17), the coefficients  $A_4$  and  $A_5$  of Tables 2 and 5 represent, respectively, the multiplier and exponent ( $\eta$ ) of the second anomalous term. Often  $\sigma_4$  is the same order of magnitude as  $A_4$ , indicating that this second term is not required by the data.

**Numerical Derivative Method (NDM)**

Table 6 contains the complete NDM results for ethylene A to compare with Tables 2, 3, and 5. Note the increase of  $\sigma_\theta$  as the number of data points decrease from thirty-

four ( $\tau \leq 0.060$ ) to nine ( $\tau \leq 0.016$ ) but the relative constancy of  $\theta$  which is always within one standard deviation of  $\bar{\theta} = 0.221$  (Table 7). Figure 3 illustrates the linearity of  $\ln(\psi_{co} + D_R)$  vs.  $\ln \tau$  for data ranges of  $\tau \leq 0.060$ ,  $\tau \leq 0.034$ , and  $\tau \leq 0.016$ . The figure contains only the data points nearest  $T_c$  (which provide the maximum deviation from linearity).

Complete NDM results for carbon dioxide A and B, ethane, ethylene B, methane, water A, and water B are

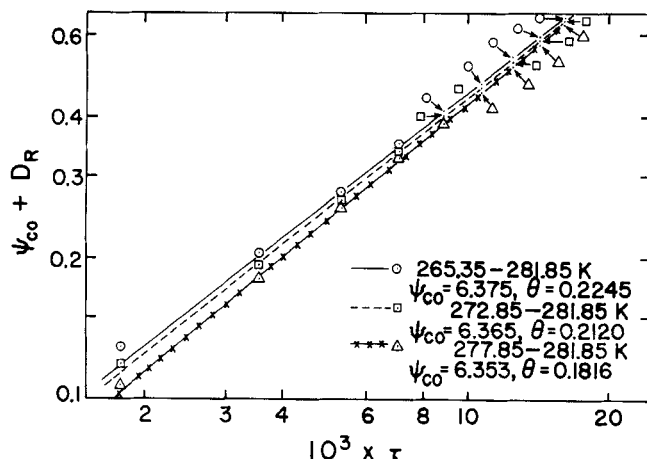


Fig. 3. Reduced vapor pressure slope for ethylene A ( $T_c = 282.35$  K,  $P_c = 5\,041.97$  kPa). Legend shows temperature ranges corresponding to Table 6.

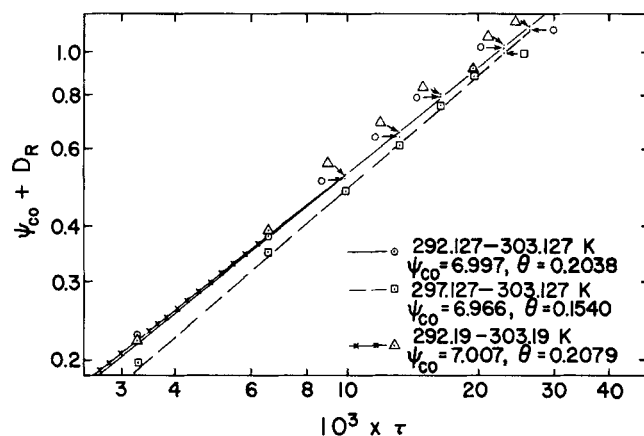


Fig. 4. Reduced vapor pressure slope for carbon dioxide A ( $T_c = 304.127$  K,  $P_c = 7\,375.3$  kPa, circles and squares) and carbon dioxide B ( $T_c = 304.19$  K,  $P_c = 7\,386.0$  kPa, triangles). The circles are from twelve data points with  $\sigma_\theta = 0.0280$ ; squares—seven data points— $\sigma_\theta = 0.0985$ , and triangles—twelve data points— $\sigma_\theta = 0.0259$ .

in the supplemental material. Figures 4 to 9 and Table 7 provide the more important results for these respective data sets. NDM analysis failed for both helium A and helium B. The scatter in the vapor pressure data of helium A caused the interpolation routine to fail, while the derivative data of helium B failed to provide a reasonable fit to any line, regardless of the choice of  $\psi_{co}$ . Likewise, scatter in both the oxygen A and oxygen B measurements caused the interpolation routine to fail.

Because not all the lines, representing different ranges of temperature, could be placed on Figures 4 to 9, a summary of  $\theta$  results follows. The weighted average value of  $\theta$  of 0.206 was within one standard deviation for all the determinations for various temperature ranges for both carbon dioxide A and B. With eight determinations for ethane,  $\bar{\theta}$  is 0.218, which is within three standard deviations of each  $\theta$ . The six determinations of ethylene B provide a  $\bar{\theta}$  of 0.205 or within four standard deviations of each  $\theta$ . All three methane determinations are shown on Figure 7, with  $\bar{\theta}$  of 0.229 within one standard deviation of each  $\theta$ . The same five determinations were made with water B as for water A with similar results. The weighted average value of 0.240 was within one standard deviation

14	9
$0.002 \leq \tau \leq 0.02$	$0.002 \leq \tau \leq 0.015$
0.221 (0.034)	0.181 (0.058)
6.370	6.353
6.07	2.62
0.80	0.71

TABLE 7. SUMMARY OF THE WEIGHTED AVERAGE VALUES  $\bar{\theta}$  WITH AVERAGE STANDARD DEVIATIONS  $\sigma_{\bar{\theta}}$  IN PARENTHESES

Compound	NLS	ML	NDM
Carbon dioxide A	0.263 (0.101)		0.200 (0.046)
Carbon dioxide B			0.207 (0.011)
Ethane	0.235 (0.066)	0.197 (0.030)	0.218 (0.048)
Ethylene A	0.221 (0.047)	0.192 (0.004)	0.221 (0.019)
Ethylene B	0.229 (0.019)	0.233 (0.049)	0.205 (0.051)
Helium A	0.093 (0.037)		
Methane	0.248 (0.063)		0.229 (0.014)
Oxygen A	0.258 (0.063)		
Oxygen B	0.258 (0.063)		
Water A			0.228 (0.074)
Water B	0.318 (0.052)		0.245 (0.046)
Weighted average	0.221 (0.064)	0.192 (0.041)	0.217 (0.047)

Overall weighted average: 0.199 (0.052).

Overall numerical average: 0.225 (0.045).

of all ten values. Unlike the CFM, the average absolute percent deviation generally increases as the temperature range narrows (ethane and ethylene B are exceptions). Also of interest is how  $\theta$  changes as the temperature range narrows to too few data points ( $\theta$  can oscillate, decrease monotonically, or increase monotonically). Ethylene A and methane oscillate; carbon dioxide A and B, ethane, and ethylene B each decrease; water A and B increase.

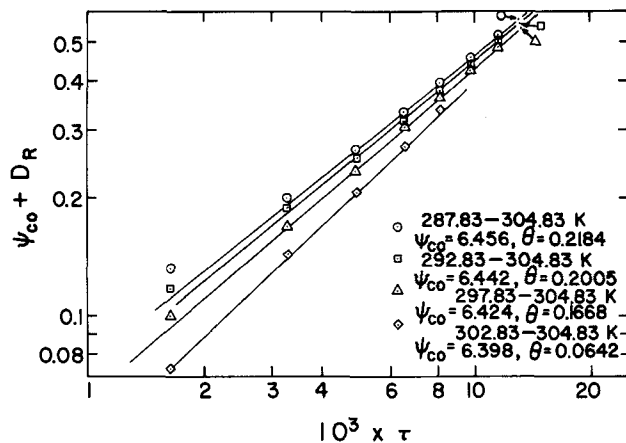


Fig. 5. Reduced vapor pressure slope for ethane ( $T_c = 305.33$  K,  $P_c = 4871.76$  kPa): The circles are from thirty five data points with  $\sigma_{\theta} = 0.0039$ ; squares—twenty five data points— $\sigma_{\theta} = 0.0076$ ; triangles—fifteen data points— $\sigma_{\theta} = 0.0215$ , and diamonds—five data points— $\sigma_{\theta} = 0.1419$ .

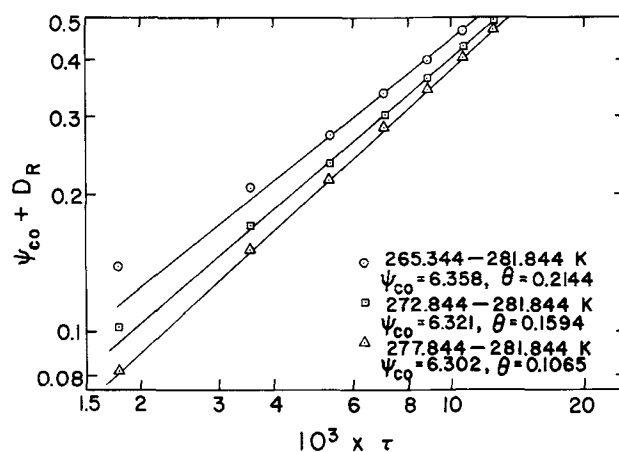


Fig. 6. Reduced vapor pressure slope for ethylene B ( $T_c = 282.344$  K,  $P_c = 5039.0$  kPa): The circles are from thirty four data points with  $\sigma_{\theta} = 0.0073$ ; squares—nineteen data points— $\sigma_{\theta} = 0.0365$ , and triangles—nine data points— $\sigma_{\theta} = 0.0303$ .

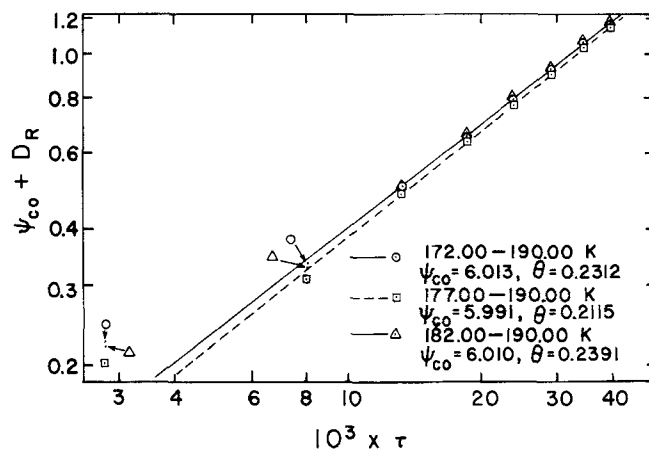


Fig. 7. Reduced vapor pressure slope for methane ( $T_c = 190.53$  K,  $P_c = 4595.7$  kPa): The circles are from nineteen data points with  $\sigma_{\theta} = 0.0091$ ; squares—fourteen data points— $\sigma_{\theta} = 0.0227$ , and triangles—nine data points— $\sigma_{\theta} = 0.0725$ .

## DISCUSSION

### Factors Affecting $\theta$

Obviously, the critical temperature and critical pressure influence  $\theta$ . However, comparison of the results from Equation (13\*) with those from Equation (13), as in



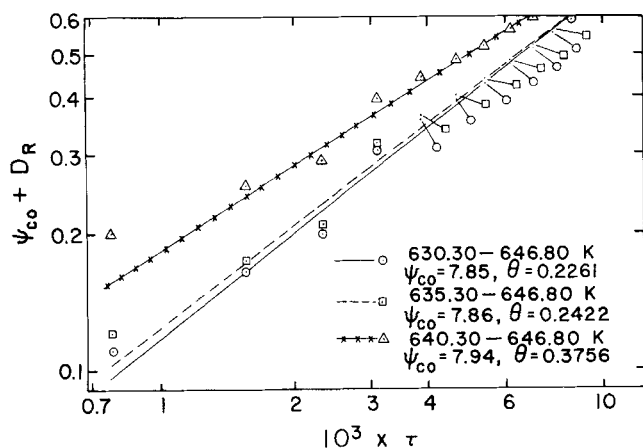


Fig. 8. Reduced vapor pressure slope for water A ( $T_c = 647.30$ ,  $P_c = 22128.7$  kPa): The circles are from thirty four data points with  $\sigma_\theta = 0.0295$ ; squares—twenty four data points— $\sigma_\theta = 0.0826$ , and triangles—fourteen data points— $\sigma_\theta = 0.3344$ .

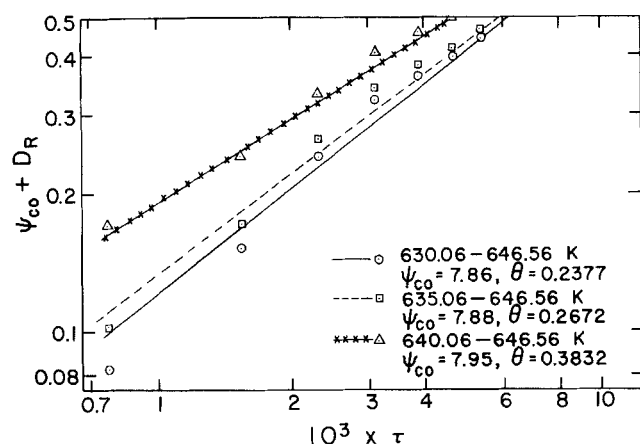


Fig. 9. Reduced vapor pressure slope for water B ( $T_c = 647.06$  K,  $P_c = 22062$  kPa): The circles are from thirty-four data points with  $\sigma_\theta = 0.0342$ ; squares—twenty-four data points— $\sigma_\theta = 0.0941$ , and triangles—fourteen data points— $\sigma_\theta = 0.3308$ .

Table 5, has shown that small changes of  $T_c$  up to four parts in 10 000 have little effect, while changes of ten parts per 10 000 will alter  $\theta$ . In both cases,  $P_c$  is adjusted (by  $\psi_c$ ) to remain on the vapor pressure curve. Slight variation of  $P_c$  holding  $T_c$  fixed causes significant changes in  $\theta$  as expected. Here, variation of  $P_c$  by one part in 10 000 and even one part in 100 000 altered  $\theta$  by several percent.

The temperature range (or maximum  $\tau$ ) was found to have a significant effect on  $\theta$  regardless of the method (CFM or NDM) or the equation assumed in the CFM. The NDM results of Table 6 for ethylene A are an example of the ideal case; the values of  $\theta$  merely scatter as data points farthest from CP are removed, and  $\sigma_\theta$  increases. The NDM results for methane and the NLS results with Equation (15) for methane, ethylene A, and oxygen B, also exhibit this behavior. Another common behavior is for  $\theta$  to drift lower with diminishing temperature range but with  $\sigma_\theta$  also increasing sufficiently to stay within three standard deviations of the highest  $\theta$ . All the remaining NDM results exhibited this behavior with  $\theta$  increasing for water A and B. Also, oxygen A and helium A ( $\theta$  increasing) from the NLS with Equation (15) showed this trend. Finally, carbon dioxide A, ethane, and ethylene B with Equation (15) exhibited decreasing values of  $\theta$ , with standard deviations remaining sufficiently small that the trend may be significant. The values of  $\theta$  for the most

narrow temperature band were 0.12, 0.23, and 0.21 for the three compounds, respectively. Equation (15) contains only one anomalous term, and a decrease of the apparent  $\theta$  with reduction of data points is expected.

The results have shown conclusively that  $\theta$  does depend on the equation selected with the CFM. The failure of Equation (17) to converge (except for ethylene A) with either NLS or ML is surprising because Hastings and Levelt Sengers (1977) have found  $\theta$  to be in the range of 0.085 to 0.125 for ethylene B. Hastings (1977) has communicated to us a fit of ethylene A with Equation (17) yielding  $\theta = 0.13$ , in close agreement with Table 2. Possible reasons why these workers are able to converge Equation (17) whereas we cannot are difference of weighting factors and difference of temperature range. In particular, they fit vapor pressure and critical isochore data simultaneously for roughly  $|\tau| < 0.1$ . The critical isochore has little or no curvature, while the vapor pressure curves considerably and definitely diverges at the CP. Therefore, their procedure should promote convergence of Equation (17) and decrease the value of  $\theta$ . The principal problem with Equation (17), however, is inclusion of the quadratic background term  $\tau^2$  which tends to blur the leading anomalous term  $\tau^{2-\theta}$ . The CFM program cannot distinguish between  $\tau^2$  and  $\tau^{1.8}$  and provide multipliers for these terms with reasonable standard deviations  $\sigma_4$  and  $\sigma_2$ , respectively (see Tables 2 and 5).

Standard deviations for both the exponents  $\sigma_\theta$  and  $\sigma_n$  and for the multipliers  $\sigma_i$  have been used extensively in this work to indicate whether the exponents and multipliers are meaningful. Low standard deviations and low absolute average percent deviations are necessary but not sufficient criteria for unique determination of  $\theta$  or the correct vapor pressure equation. Error bands placed on  $\theta$  should reflect two or three standard deviations (95 and 99% confidence limits).

#### The Value of $\theta$

Table 7 supports the contention that  $\theta$  is a universal constant  $\sigma_\theta$ . Removal of these two compounds from the NLS results provides  $\bar{\theta} = 0.234$  with  $\sigma_\theta = 0.020$ . Our final recommended value of  $\theta$  is  $0.22 \pm 0.04$  with helium A and water B providing exceptions. The low value of helium A also conflicts with a rough study of helium B by the NDM. While the scatter of the direct measurement of vapor pressure slope by Kierstead (1971) is sufficient to cause failure of fit via Equation (21), graphs similar to Figures 3 to 9 can be prepared for different values of  $\psi_c$ . An approximate  $\psi_{co}$  of 3.9360 provides a straight line with a slope of 0.825 or  $\theta = 0.175$ . The data appear to scatter randomly about this line. Use of  $\psi_c = 3.9302$  from Kierstead's analysis provides a convex upwards curve with  $\theta$  negative for the temperature range of the last four data points. Uncertainties in the practical temperature scales are far more significant for helium than for the other substances considered here. The high values of  $\bar{\theta}$  for water B (NLS) may be due to the extended temperature range as  $\tau = 0.1$  corresponds to 64.7 deg below the CP.

#### Theoretical Comparisons

A  $\theta$  of  $0.22 \pm 0.04$  is too high to equal the isochoric heat capacity exponent  $\alpha$  ( $1/8$ ) from the lattice gas model. Experimental values of  $\alpha$  have risen historically from zero in the early 1960's to near ( $1/8$ ) currently with 0.15 (Moldover, 1969) for  $^4\text{He}$  as one of the highest values.

Likewise,  $\theta = 0.22 \pm 0.04$  is too low to equal  $(1-2\beta)$  or 0.29 if  $\beta = 0.355$ . The latter value of  $\beta$  was widely accepted until recently, when Hocken and Moldover

(1976) obtained values of near 0.32 from analysis of their optical measurements, and Hall and Eubank (1976) proved that  $\beta$  equals  $\beta'$  (the critical exponent of the heat of vaporization) lest the Clapeyron equation be violated. Values of  $\beta'$  range from 0.35 to 0.41, with  $(\frac{3}{8})$  as an average. Because the heat of vaporization is linear with  $\tau$  on a logarithmic graph to  $\tau = 0.1$ , whereas the orthobaric density difference is not, determinations of  $\beta'$  are little affected by higher-order terms.

A consistent set of critical exponents based upon experiment is then  $\beta = \frac{3}{8}$ ,  $\theta = 1 - 2\beta = \frac{1}{4}$ ,  $\lambda = 1 - \alpha - \beta = (\frac{1}{2})$ ,  $\gamma = 1 + \lambda - \beta = (9/8)$ , and  $\delta = [(\lambda + 1)/\beta] = 4$ . The weak singularity of  $\tau^{3-2(\alpha+\beta)}$  predicted by Nicoll et al. (1975) for the critical isochore is removed with the isochore parabolic. These rough, apparent exponents should be useful in correcting equations of state used in engineering calculations and the construction of thermodynamic property tables for the critical region.

## ACKNOWLEDGMENT

Dr. Patrick J. White, Research Associate, developed and operated the maximum likelihood program. Financial support was provided by the National Science Foundation (ENG-76-00692 and ENG-77-01070), American Gas Association (BR110-1, BR110-2), Petroleum Research Fund (7594-AC7), and the Texas Engineering Experiment Station.

## NOTATION

- $k_{A_j}$  = general coefficients determined by minimization of the objective function in the CFM  
 $B_1, B_2$  = coefficients determined by the NDM  
 $C_j$  = initial coefficients  
 $C_V$  = isochoric heat capacity  
 $D_o$  = analytic, background function of temperature  
 $D_j, E$  = coefficients in the equation of Hastings and Levelt Sengers  
 $D_R$  = vapor pressure slope,  $dP_{\sigma R}/d\tau$   
 $E_o, F_o$  = coefficients for the anomalous terms of Equation (8)  
 $M$  = number of free parameters to be found in a particular equation  
 $N$  = total number of data points  
 $P$  = pressure, kPa  
 $T$  = temperature, K  
 $V$  = specific volume,  $m^3/kg\text{-mol}$   
 $W$  = weighting factor defined by Equation (22)

## Greek Letters

- $\alpha$  = critical exponent of the isochoric heat capacity  
 $\beta$  = critical exponent of the orthobaric density difference  
 $\gamma$  = critical exponent of the isothermal compressibility  
 $\Delta$  = difference between experimental and calculated value  
 $\delta$  = critical exponent of the critical isotherm  
 $\eta$  = second order critical exponent of the vapor pressure curvature  
 $\theta$  = primary critical exponent of the vapor pressure curvature  
 $\bar{\theta}$  = weighted average value of  $\theta$   
 $\mu$  = chemical potential,  $kPa\text{-m}^3/kg\text{-mol}$   
 $\rho$  = density,  $kg\text{-mol}/m^3$   
 $\sigma_i$  = standard deviation of the coefficient  $k_{A_i}$   
 $\sigma_x$  = standard deviation of the quantity  $x$   
 $\tau$  = reduced temperature,  $(T_c - T)/T_c$   
 $\psi_c$  = dimensionless slope of vapor pressure curve at the CP, see Equation (7)  
 $\psi_{co}$  = optimum value of  $\psi_c$

## Subscripts

- $c$  = critical point  
 $eq$  = value calculated from the equation  
 $i$  = data point counter  
 $j$  = coefficient counter  
 $R$  = reduced or dimensionless  
 $\sigma$  = experimental value along the coexistence curve

## Superscripts

- $k$  = counter denoting particular vapor pressure equation  
 $\bullet$  = combined coefficients of Equation (10)

## LITERATURE CITED

- Baehr, H. D., H. Garnjost, and R. Pollak, "The Vapor Pressure of Liquid Ammonia—New Measurements above 328 K and a Rational Vapor-pressure Equation," *J. Chem. Thermo.*, **8**, 113 (1976).  
Blank, G., "Neue Bestimmung des Kritischen Punktes von leichtem und schwerem Wasser," *Warme-Stoffuebertragung*, **2**, 53 (1969).  
Britt, H. I., and R. H. Luecke, "The Estimation of Parameters in Non-Linear, Implicit Models," *Technometrics*, **15**, 233 (1973).  
Douslin, D. R., and R. H. Harrison, "Pressure, Volume, Temperature Relations of Ethane," *J. Chem. Thermo.*, **5**, 491 (1973).  
———, "Pressure, Volume, Temperature Relations of Ethylene," *ibid.*, **8**, 301 (1976).  
Gielen, H., V. Jansoone, and O. Verbeke, "Application of an Empirical Equation of State to the Critical Region of Methane and Argon," *J. Chem. Phys.*, **59**, 5763 (1973).  
Goodwin, R. D., "Nonanalytic Vapor Pressure Equation with Data for Nitrogen and Oxygen," *J. Res. Natl. Bur. Stand.*, **73A**, 487 (1969).  
———, "Equation of State for Thermodynamic Properties of Fluids," *ibid.*, **79A**, 71 (1975).  
Griffiths, R. B., "Ferromagnets and Simple Fluids near the Critical Point: Some Thermodynamic Inequalities," *J. Chem. Phys.*, **43**, 1958 (1965).  
Hall, K. R., and P. T. Eubank, "Empirical Description of the Liquid-Vapor Critical Region based on Coexistence Data," *Ind. Eng. Chem. Fundamentals*, **15**, 323 (1976).  
Hastings, J. R., and J. M. H. Levelt Sengers, "Vapor Pressure, Critical Pressure, and Critical Isochore of Ethylene," *Proceedings of the Seventh Symposium on Thermophysical Properties*, Am. Soc. Mech. Eng., pp. 794-806 (May, 1977).  
Hastings, J. R., private communication (May 20, 1977).  
Hildebrand, F. B., *Introduction to Numerical Analysis*, 2 ed., McGraw-Hill, New York (1974).  
Hocken, R., and M. R. Moldover, "Ising Critical Exponents in Real Fluids: An Experiment," *Phys. Rev. Lett.*, **37**, 29 (1976).  
Hoge, H. J., "Vapor Pressure and Fixed Points of Oxygen and Heat Capacity in the Critical Region," *J. Res. Natl. Bur. Stand.*, **44**, 321 (1950).  
Hust, J. G., and R. D. McCarty, "Curve-Fitting Techniques and Applications to Thermodynamics," *Cryogenics*, **7**, 200 (1967).  
Jansoone, V., H. Gielen, J. DeBoelpaep, and O. B. Verbeke, "The Pressure-Temperature-Volume Relationships of Methane near the Critical Point," *Physica*, **46**, 213 (1970).  
Kierstead, H. A., "Pressures on the Critical Isochore of He<sup>4</sup>," *Phys. Rev.*, **A3**, 329 (1971).  
Kim, D. M., D. L. Henry, and R. Kobayashi, "Effects of Density Gradients on Measurements of the Decay Rate of Spontaneous Density Fluctuations in Fluids Near the Critical Point," *ibid.*, **A10**, 1808 (1974).  
Levelt Sengers, J. M. H., "Scaling Predictions for Thermodynamic Anomalies Near the Gas-Liquid Critical Point," *Ind. Eng. Chem. Fundamentals*, **9**, 470 (1970).  
———, and W. T. Chen, "Vapor Pressure, Critical Isochore, and Some Metastable States of CO<sub>2</sub>," *J. Chem. Phys.*, **56**, 595 (1972).  
Levelt Sengers, J. M. H., R. Hocken, and J. V. Sengers,

- "Critical-Point Universality and Fluids," *Physics Today*, 42 (Dec., 1977).
- Moldover, M. R., "Scaling of the Specific-Heat Singularity of  $\text{He}^4$  Near Its Critical Point," *Phys. Rev.*, **182**, 342 (1969).
- , "Visual Observation of the Critical Temperature and Density:  $\text{CO}_2$  and  $\text{C}_2\text{H}_4$ ," *J. Chem. Phys.*, **61**, 1766 (1974).
- Moursund, D. G., and C. S. Duris, *Elementary Theory and Application of Numerical Analysis*, McGraw-Hill, New York (1967).
- Nicoll, J. F., T. S. Chang, A. Hankey, and H. E. Stanley, "Scaling Laws for Fluid Systems Using Generalized Homogeneous Functions of Strong and Weak Variables," *Phys. Rev.*, **B11**, 1176 (1975).
- Nuckols, J. W., "A New Vapor Pressure Equation Originating at the Critical Point," M.S. thesis, Texas A&M Univ., College Station (1976). (Paper presented at the 69th Annual Mt., AIChE, Paper 54f-Fiche No. 43, Chicago, November, 1976).
- Osborne, N. S., H. F. Stimson, E. F. Fiock, and D. C. Ginnings, "The Pressure of Saturated Water Vapor in the Range  $100^\circ$  to  $374^\circ\text{C}$ ," *J. Res. Natl. Bur. Stand.*, **10**, 155 (1933).
- Osborne, N. S., H. F. Stimson, and D. C. Ginnings, "Thermal Properties of Saturated Water and Steam," *ibid.*, **23**, 261 (1939).
- Prydz, R., and R. D. Goodwin, "Experimental Melting and Vapor Pressures of Methane," *J. Chem. Thermo.*, **4**, 127 (1972).
- Rehr, J. J., and N. D. Mermin, "Revised Scaling Equation of State at the Liquid-Vapor Critical Point," *Phys. Rev.*, **A8**, 472 (1973).
- Roach, P. R., "Pressure-Density-Temperature Surface of  $\text{He}^4$  near the Critical Point," *ibid.*, **170**, 213 (1968).
- Rowlinson, J. S., *Handbuch der Physik*, S. Flügge, ed., Vol. XII, p. 17, Springer-Verlag, Berlin, Germany (1958).
- Stanley, H. E., *Introduction to Phase Transitions and Critical Phenomena*, Oxford University Press, New York (1971).
- Verbeke, O. B., "An Equation for the Vapor Pressure Curve," *Cryogenics*, **10**, 486 (1970).
- Vincentini-Missoni, M., J. M. H. Levelt Sengers, and M. S. Green, "Scaling Analysis of Thermodynamic Properties in the Critical Region of Fluids," *J. Res. Natl. Bur. Stand.*, **73A**, 563 (1969).
- Wagner, W., J. Ewers, and W. Pentermann, "New Vapour-Pressure Measurements and a New Rational Vapour-Pressure Equation for Oxygen," *J. Chem. Thermo.*, **8**, 1049 (1976).
- Walton, C. W., "Optimal Determination of the Vapor Pressure Critical Exponent," M.S. thesis, Texas A&M Univ., College Station (1977).
- Wegner, F. J., "Corrections to Scaling Laws," *Phys. Rev.*, **B5**, 4529 (1972).
- Widom, B., and J. S. Rowlinson, "New Model for the Study of Liquid-Vapor Phase Transitions," *J. Chem. Phys.*, **52**, 1670 (1970).
- Yang, A. J. M., P. D. Fleming, and J. H. Gibbs, "Theory of the Influence of Gravity on Liquid Vapor Interfaces," *ibid.*, **67**, 74 (1977).
- Yang, C. N., and C. P. Yang, "Critical Point in Liquid-Gas Transitions," *Phys. Rev. Lett.*, **13**, 303 (1964).
- Young, H. D., *Statistical Treatment of Experimental Data*, McGraw-Hill, New York (1962).

Manuscript received January 23, 1978; revision received July 12, and accepted July 18, 1978.

# An Approximate Theory of Interfacial Tensions of Multicomponent Systems: Applications to Binary Liquid-Vapor Tensions

P. H. WINTERFELD

L. E. SCRIVEN

and

H. T. DAVIS

Department of Chemical Engineering  
and Materials Science  
University of Minnesota  
Minneapolis, Minnesota 55455

Formulas obtained by approximation of the rigorous expression for the interfacial tension of multicomponent, polyatomic fluids are shown to provide accurate and simple estimates of the composition dependence of the surface tension of nonaqueous, binary solutions at low vapor pressures. Similar formulas are recommended for multicomponent (that is, more than two components) solutions.

## SCOPE

From the Fowler model (1937) [also known as the Fowler-Kirkwood-Buff (1949) model], an expression is obtained relating interfacial tension of multicomponent systems to quantities dependent on intermolecular pair

Correspondence concerning this paper should be addressed to H. T. Davis.

0001-1541/78-1685-1010-\$00.75. © The American Institute of Chemical Engineers, 1978.

potential and pair correlation functions. As a special case, a simple formula is obtained, relating surface tension to composition at low vapor pressures. This formula, like Eberhart's (1966) and others, involves a parameter that is difficult to determine theoretically, since pair potential and correlation functions are not generally available. This parameter was determined by a simplified model and by fitting experimental data.